Theoretical and Applied Climatology (2025) 156:295
https://doi.org/10.1007/s00704-025-05533-9

RESEARCH

Climate change impacts on hydrological and meteorological variables in Diyarbakır Province: trend analysis and machine learning-based drought forecasting

Ergun Akbas[1] · Recep Çelik[2] · Musa Esit[3] · Ibrahim Halil Deger[4]

Received: 27 March 2025 / Accepted: 29 April 2025

Abstract
This study examines the effects of climate change using monthly precipitation, evapotranspiration, temperature, relative humidity, and streamflow data (1963–2021) obtained from meteorological and hydrological stations in the city center of Diyarbakır. For trend analysis, Mann–Kendall (MK) test, Sen's Slope Test (SS), and Innovative Polygon Trend Analysis (IPTA) methods were applied, and the results were compared. The study evaluates the performance of these methods in different climate variables, showing that statistically significant trends in precipitation, temperature, humidity, evaporation, and flow variables occur in certain months in Diyarbakır. The findings provide an important data source for water resource management and drought risk assessments. Additionally, drought analyses were performed using the Standardized Precipitation Index (SPI), Standardized Precipitation-Evapotranspiration Index (SPEI), and Streamflow Drought Index (SDI), and SDI predictions were made using machine learning techniques such as Multilayer Perceptron (MLP), Linear Regression (LR), Support Vector Machines (SVM), and Random Forest (RF) algorithms. The algorithm providing the best prediction performance was determined.

1 Introduction

In recent years, a significant increase in the frequency of extreme weather events has been observed, with climate change identified as the primary cause (Bellprat et al. 2019; Ayugi et al. 2022). According to the Katherine et al. (2023) as noted in the IPCC (2013b), the rise in atmospheric temperature has deepened concerns about global warming. Studies published by the IPCC (2013a, 2014) emphasize the widespread and varied impacts of climate change across all geographical regions, including arid, semi-arid, and humid areas. In this context, a precise understanding of precipitation and temperature mechanisms is crucial for preventing climate-related disasters and mitigating their adverse effects (Kesgin et al. 2024).

Drought is a natural disaster characterized by prolonged and unusual deficiencies in precipitation (Mohseni Saravi et al. 2009). It arises when long-term water demand exceeds the available supply and typically develops slowly over an extended period (Wilhite et al. 2007; Dubrovsky et al. 2009). To better understand the impacts of drought, various meteorological and hydrological drought indices are used. Indices like the Standardized Precipitation Index (SPI), the Standardized Precipitation-Evapotranspiration Index (SPEI) and Standardized Drought Index (SDI) are widely employed to identify and compare drought events (McKee et al. 1993; Vicente-Serrano et al. 2010; Abro et al. 2022; AghaKouchak et al. 2022). Research consistently shows that droughts are becoming more frequent and intense, which emphasizes

✉ Musa Esit
mesit@adiyaman.edu.tr

Ergun Akbas
ergunakbas@gmail.com

Recep Çelik
recep.celik@dicle.edu.tr

Ibrahim Halil Deger
ibrahim.deger@hku.edu.tr

[1] General Directorate of State Hydraulic Works, Adıyaman, Türkiye

[2] Department of Civil Engineering, Dicle University, Diyarbakır, Türkiye

[3] Department of Civil Engineering, Adıyaman University, Adıyaman, Türkiye

[4] Civil Engineering Department, Hasan Kalyoncu University, Gaziantep, Türkiye

Published online: 09 May 2025

the critical need for reliable methods to assess and predict drought changes and thereby reduce their impact (Adarsh et al. 2018; Aksoy and Cavus 2022; Avsaroglu and Gumus 2022). Researchers have historically used these indices to quantify drought duration, intensity, and frequency, examining their temporal and spatial distribution (Esit et al. 2021; Kundu et al. 2024; Bera and Dutta 2024; Kumar et al. 2024).

Climate change is driving a rise in the frequency and intensity of extreme events like droughts, largely through shifts in global precipitation and temperature. Consequently, it's critical to analyze meteorological variables using both traditional Mann–Kendall (MK) and novel techniques, such as the Innovative Polygon Trend Analysis (IPTA) method (Şen et al. 2019; Achite et al. 2021; Esit 2022; Qadem and Tayfur 2024). This trend assessment is essential for effective drought management and informed decision-making regarding necessary precautions.

To analyze trends in hydro-meteorological data, Şen (2012) proposed the Innovative Trend Analysis (ITA). To further validate these trends, the Innovative Trend Significance Test (ITST) was developed by Şen (2017). Expanding upon these, Şen et al. (2019) introduced the IPTA, enabling the analysis of temporal changes within time series. The global adoption of IPTA is evident in the numerous studies applying it to diverse hydro-meteorological parameters (Boudiaf et al. 2022; Sezen 2023; Koycegiz and Buyukyildiz 2024; Kartal and Emiroglu 2024). The graphical methods demonstrated superior accuracy in identifying hidden trends compared to traditional methods, as shown by a comparative analysis of various hydro-climatic datasets (Dabanlı et al. 2016; Boudiaf et al. 2022; Sezen 2023; Qadem and Tayfur 2024; Şan 2025).

Developing long-term strategies to address global warming-induced water scarcity and accurately predict droughts is essential (Soh et al. 2018; Alahacoon and Edirisinghe 2022). Drought prediction can be achieved through physical/conceptual or data-driven models. While physical/conceptual models are valuable for understanding catchment dynamics, they face criticism for their complexity, extensive data requirements, and challenges in forecasting applications. Machine learning (ML) has recently become a focal point of research across diverse fields, including engineering, agriculture, medicine, marketing, and earth and environmental sciences (Belayneh et al. 2016; Achite et al. 2022; Firdaus et al. 2023; Tuğrul et al. 2025). Despite the complexity and uncertainty that make drought forecasting difficult (Durbach et al. 2017), it remains vital for reducing drought risks. Machine learning (ML) stands out as a powerful solution because it can operate effectively even with minimal amounts of data. A considerable amount of empirical research has been noted to using traditional regression alongside data-driven techniques with an emphasis on ML for predicting drought indices (Jehanzaib et al. 2021; Aghelpour et al. 2021; Prodhan et al. 2022; Karbasi et al. 2023; Oruc et al. 2024; Elbeltagi et al. 2024; Pande et al. 2024; Latifoğlu et al. 2024; Alkubaisi et al. 2024; Tuğrul and Hinis 2025).

In this study, the effects of climate change were examined using meteorological and hydrological data from Diyarbakır province. Diyarbakır, one of the prominent provinces in the Southeastern Anatolia Region of Turkey, stands out for its rich water resources and biodiversity. Ensuring the sustainable preservation of water resources and accurately predicting climate-induced disasters and taking necessary precautions are of great importance in this region. Traditional methods such as the MK test and Sen's Slope Test (SS), along with the Innovative approach IPTA method, were applied for trend analysis. Ultimately, drought analyses were conducted using the SPI, SPEI, and SDI. Furthermore, machine learning algorithms were employed to predict the SDI, aiming to contribute to the management of climate change-induced trends and drought risk in Diyarbakır.

2 Methodology

2.1 Mann–Kendall (MK) test

The Mann–Kendall test (Mann 1945; Kendall 1975) is a non-parametric and distribution-free method widely used for trend analysis in hydro-meteorological time series. This test detects increasing or decreasing trends by calculating the Z_{MK} value, as shown in Eq. 4. Positive Z_{MK} values indicate an increasing trend, while negative values indicate a decreasing trend. If $|Z_{MK}| > |Z\alpha/2|$, the trend is considered statistically significant. This method is commonly applied with a 95% confidence interval to determine strong trends (Saplıoğlu 2024). The procedures used to calculate the Mann–Kendall (Z) value have been extensively discussed in the literature (Ashraf et al. 2021; Esit et al. 2023; Gaddikeri et al. 2024) and were similarly applied in this study. The test statistic S is evaluated as follows:

$$S = \sum_{k=1}^{n-1} \sum_{j=k+1}^{n} sgn(x_j - x_k) \tag{1}$$

where n indicates the number of the data, t_i is represented as the length of the tied rank group and x_j and x_k show the data point in years j and k (j > k).

$$sgn(x_j - x_k) = \begin{cases} 1(x_j - x_k) > 0 \\ 0(x_j - x_k) = 0 \\ -1(x_j - x_k) < 0 \end{cases} \tag{2}$$

$$Var(S) = \frac{n(n-1)(2n+5) - \sum_i^r t_i(t_i-1)(2t_i+5)}{18} \tag{3}$$

$$Z = \begin{cases} \frac{S-1}{\sqrt{Var(S)}} S > 0 \\ 0 S = 0 \\ \frac{S+1}{\sqrt{Var(S)}} S < 0 \end{cases} \quad (4)$$

2.2 Sen's Slope (SS) estimator

The Sen's Slope Estimator (Sen 1968) is a non-parametric technique used to determine the slope of a trend in a given dataset. The slope is calculated as the median of the differences in slopes between all data points. Developed by Sen (1968), this method is particularly suitable for trend analysis in equally spaced time series. The slope calculation procedure involves computing the differences between data pairs, ranking them, and identifying the median value (Helsel and Hirsch 2002).

$$S = \frac{Q_2 - Q_1}{T_2 - T_1} \quad (5)$$

$$S = \begin{cases} S_{\frac{n+1}{2}} & n = even \\ S_{\frac{n}{2}} & n = odd \end{cases} \quad (6)$$

2.3 Innovative Polygon Trend Analysis (IPTA)

The Innovative Polygon Trend Analysis (IPTA) method, developed by Şen et al. (2019), can be applied to daily, monthly, annual, and seasonal time series. In this study, monthly time series were utilized. For monthly precipitation data, an n-year series x_1 to x_n was used to construct the following monthly matrix.

$$\begin{bmatrix} x_{1,1} & x_{1,2} & \cdots & x_{1,12} \\ x_{2,1} & x_{2,2} & \cdots & x_{2,12} \\ \cdot & \cdot & \cdots & \cdot \\ \cdot & \cdot & \cdots & \cdot \\ \cdot & \cdot & \cdots & \cdot \\ x_{n,1} & x_{n,2} & \cdots & x_{n,12} \end{bmatrix} \begin{matrix} Upper\ series \\ (First\ Half) \\ i = 1,2,3,\ldots\ldots\ldots,n/2 \\ \hline Lower\ series \\ (Secon\ Half) \\ i = n/2+1, n/2+2,\ldots\ldots..,n \end{matrix} \quad (7)$$

The monthly dataset was divided into two equal parts, and the arithmetic mean or standard deviation of each subset was calculated. Subsequently, the arithmetic mean or standard deviation of the first subset was plotted on the x-axis, while the corresponding values of the second subset were plotted on the y-axis. This representation of the monthly precipitation data using the IPTA method is illustrated in Fig. 1 (Ceribasi et al. 2021).

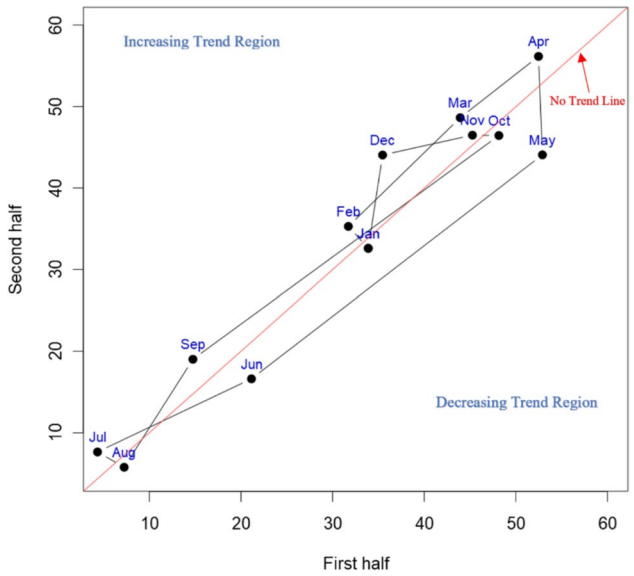

Fig. 1 A schematic representation of Innovative Polygon Trend Analysis (IPTA)

2.4 Standardized Precipitation Index (SPI)

The Standardized Precipitation Index (SPI), proposed by McKee et al. (1993), is a widely used index in drought analysis, assessing how precipitation levels in a given region deviate from the normal distribution over time. The SPI's popularity in climate research stems from several key factors, notably its simplicity and ease of use. As it relies solely on readily accessible precipitation data, researchers across various disciplines and regions find it highly applicable (Cancelliere et al. 2007; Akbari et al. 2015). Furthermore, the SPI is recommended by the World Meteorological Organization (WMO) for global implementation, as it provides a clear indication of relative precipitation over specific time intervals (Pei et al. 2020; Yalçın et al. 2023). The gamma distribution is characterized by the following frequency or probability density function:

$$g(x) = \frac{1}{\beta^{\alpha}\Gamma(a)} \times^{a-1} e^{-\frac{x}{\beta}} for x > 0 \quad (8)$$

where x represents the precipitation amount, α and β are the shape and scale parameters respectively, and Γ(α) denotes the gamma function. These parameters can be determined using Maximum Likelihood Estimation (MLE):

$$\alpha = \frac{1}{4A}\left[1 + \sqrt{1 + \frac{4A}{3}}\right], \beta = \frac{\bar{x}}{\alpha}, A = (\bar{x}) - \frac{\sum \ln(x)}{n} \quad (9)$$

where n indicates the number of observations.

The cumulative probability for a recorded precipitation event in the specified month and time frame for the given location is then computed using the selected parameters. Since the gamma distribution G(x) cannot be defined when monthly precipitation equals zero (x = 0), the cumulative probability is instead expressed as:

$$H(x)=q+(1-q)G(x) \tag{10}$$

where q represents the probability of zero rainfall, and G(x) denotes the cumulative probability of the incomplete gamma function. According to McKee et al. (1993), the basin is categorized into wetness and dryness groups based on SPI values (Table 1).

2.5 Standardized Precipitation Evapotranspiration Index (SPEI)

The SPEI, developed by Vicente-Serrano et al. (2010), is an index used for drought analysis, evaluating the balance between precipitation and potential evapotranspiration (PET). This index provides a more comprehensive analysis of water resources and agriculture, especially in cases where precipitation-based analyses are insufficient. The SPEI is determined by computing the non-exceedance probability of the difference between precipitation and potential evapotranspiration. This difference is then standardized using a three-parameter log-logistic probability distribution function. This particular distribution is essential as it can accommodate negative values, which frequently occur in the water balance calculations within the SPEI methodology (Vicente-Serrano et al. 2010; Danandeh Mehr et al. 2020). The SPEI is computed by normalizing the climatic water balance through a Log-logistic distribution. For this study, the Potential Evapotranspiration (PET) is calculated using the Thornthwaite method (Thornthwaite 1948). The primary calculation involves determining the difference (Di) between precipitation (P) and PET for a given month (i).

$$PET = 16d\left(\frac{10T}{I}\right)^{a} \tag{11}$$

Table 1 The classification of SPI, SPEI, and SDI indices

Category	Criterion
Non-Drought	SPI, SDI and SPEI ≥ 0.0
Mild drought	−1.0 ≥ SPI, SDI and SPEI < 0.0
Moderate drought	−1.5 ≥ SPI, SDI and SPEI < −1
Severe drought	−2.0 ≥ SPI, SDI and SPEI < −1.5
Extreme drought	SPI, SDI and SPEI < −2.0

T is the monthly mean temperature (°C), and d, a correction factor for monthly diurnal duration variations, is obtained from latitude-specific standard tables.

$$D_i = P_i - PET_i \tag{12}$$

The D values are summed across time scales.

$$D_n^k = \sum_{i-0}^{k-1} P_{n-1} - (PET)_{n-1} \tag{13}$$

where k notes as the aggregation period in months and n is the calculation month.

2.6 Streamflow Drought Index (SDI)

A hydrological drought is characterized by inadequate groundwater and surface water supplies, such as river flows, groundwater levels, and water in lakes and reservoirs. Assessing this type of drought involves monitoring the water levels across these sources (Nalbantis and Tsakiris 2009; Tabari et al. 2013; Jahangir and Yarahmadi 2020). This study utilizes the standardized streamflow index (SDI) (Nalbantis and Tsakiris 2009), which follows a similar concept to the SPI, to analyze hydrological drought. The flow data in Eq. 14 is denoted as Qa,b, where k represents the reference period,"a"indicates the hydrological year, and"b"signifies the month within a water year. Equation 14 demonstrates how the SDI method calculates the cumulative flow volume (Nalbantis 2008).

$$V_{a,k} = \sum_{j=1}^{3k} Q_{a,b} a = 1, 2, \ldots b = 1, 2, \ldots, 12k = 1, 2, 3, 4 \tag{14}$$

For the calculations, cumulative discharge volumes were analyzed across four periods: k = 1 (October-December), k = 2 (October–March), k = 3 (October-June), and k = 4 (October-September). The resulting Standardized Drought Index (SDI) values for each k period of the hydrological year are as follows:

$$SDI_{a,k} = \frac{V_{a,k} - \overline{V_k}}{S_k} a = 1, 2, \ldots, k = 1, 2, 3, 4 \tag{15}$$

In this equation, S_k and $\overline{V_k}$ represent the standard deviation of the cumulative flow rate during the reference period, represents the average cumulative flow rate during the reference period, and represents a specific streamflow value.

2.7 Support Vector Machine (SVM)

Support Vector Machine (SVM) is a powerful classification algorithm that uses supervised learning and kernel-based techniques. Based on a linear prediction approach, SVM has

the ability to provide multiple prediction results for a given input (Mokhtarzad et al. 2017; Zhang et al. 2020). It is a highly successful method in both binary classification problems and regression analysis (Özbeyaz and Söylemez 2020). The goal is to ensure accurate data parsing during classification. This decomposition method employs linear boundaries and can generate an unlimited number of lines. It utilizes a margin—a defined range—to determine the optimal separation. When establishing this margin, the widest possible range is taken into account (Zhang et al. 2020; Alkan and Tombul 2024).

$$\underset{w,b}{minf}(w,b) = \left(\frac{1}{2}\right)\|w\|^2 \tag{16}$$

$$y_i\left(w_i x_i + b\right) \geq +1,\ i = 1,...,N, \tag{17}$$

$$w_i = \sum_{i}^{N} y_i \alpha_i x_i, \tag{18}$$

where wi represent the weight vector, b shows bias and xi indicates a point on the hyperplane. The maximal margin classifier is determined using Lagrange multipliers as follows:

$$L(w,b,a) = \left(\frac{1}{2}\right)\|w\|^2 - \sum_i^N \alpha_i\left(y_i\left(<\times,\times_i> +b\right) - 1\right) \tag{19}$$

The RBF kernel is shown below:

$$K\left(x_i, x_j\right) = \exp\left(-\gamma\| x_i - x_j \|^2\right), \gamma > 0, \tag{20}$$

where γ is the bandwidth parameter of the Gaussian RBF kernel and ||xi—xjll^2 represents the squared Euclidean distance. Following the solution of the dual problem, the decision function takes the following form

$$f(x) = sgn\left(\sum_{i=1}^{N} \alpha_i y_i K < x,\ x_i > +b\right) \tag{21}$$

Only samples exhibiting non-zero Lagrange multipliers are included in the solution, and b is calculated based on the primal–dual relationship (Schölkopf and Smola 2002). Figure 2 shows the structure of SVM flowchart.

2.8 Multilayer Perceptron (MLP)

The Multilayer Perceptron (MLP) is one of the most widely used types of networks within Artificial Neural Networks (ANN). MLP processes data through multiple layers and delivers effective results, especially in tasks like classification, regression, and prediction (Prabowo et al. 2024). MLP excels at solving non-linear problems (Aghelpour and Varshavian 2021). Calculations are performed using a non-linear activation function, which is expressed as follows:

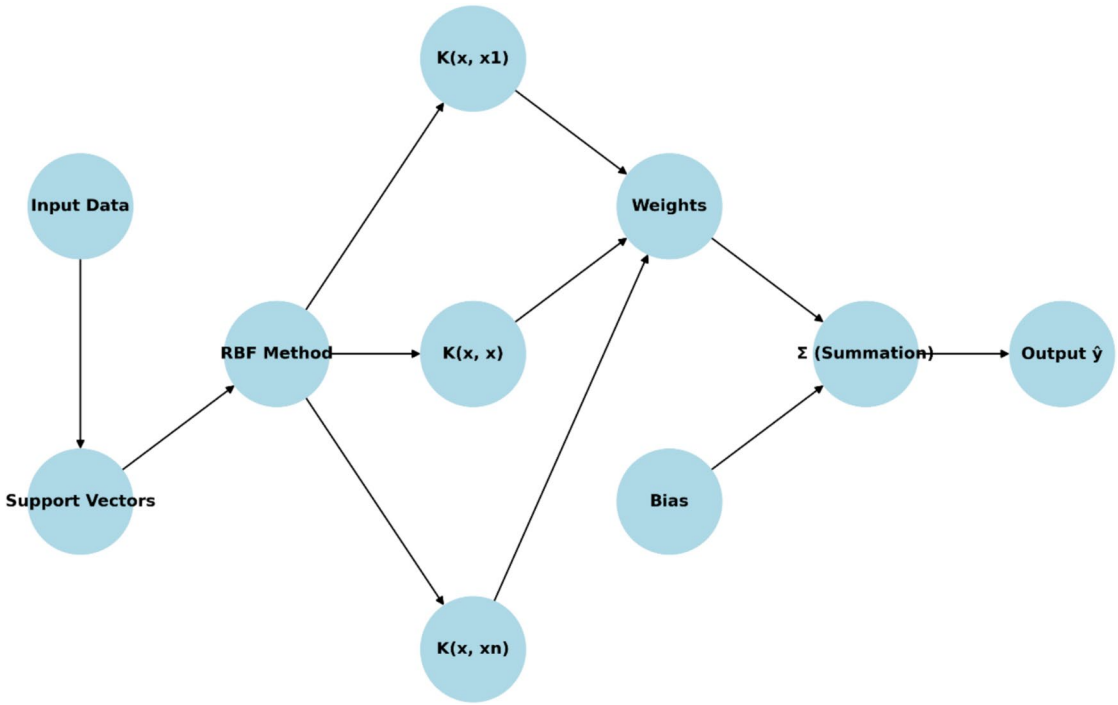

Fig. 2 Demonstration of the support vector machine flowchart

$$y = \Phi(\sum_{i=1}^{n} wixi + b) = \Phi w^T xi + b \tag{22}$$

Here,'w'represents the vector of input weights,'y'represents the input combination,'y'denotes the bias, and the activation function is represented by'Φ'. Figure 3 indicates the Multilayer perception model structure.

2.9 Random Forest (RF)

Random Forest is a powerful machine learning model used for analyzing climate data, such as meteorological variables like temperature, precipitation, and humidity(Lotfirad et al. 2021; Elbeltagi et al. 2023). This model helps identify patterns, trends, and relationships between different climate variables over time. Random Forest can be trained to predict extreme weather events, such as hurricanes, heatwaves, droughts, and heavy rainfall (Breiman 2001). By analyzing historical climate data and other factors like sea surface temperatures, atmospheric pressure, and geographical features, it provides valuable insights into the likelihood and intensity of such events in the future. Random Forest models also assess the potential impacts of climate change on ecosystems, biodiversity, agriculture, water resources, and human populations.

2.10 Evaluation model

To understand the effectiveness of our drought model, we evaluate its performance by measuring its accuracy and error. This evaluation is based on 5 specific parameters: R^2, MAE (Mean absolute error), RMSE ((Root Mean Squared Error), RAE (Relative Absolute Error) and RRSE (The Root Relative Squared Error). The RMSE typically measures the differences between samples of data, or all data values. For each of the distinct samples T, the RMSE of the predicted values for the dependent variable x_t is computed using variables expected across sample periods (Alkan and Tombul 2024). MAE measures the difference between predicted and observed data. Importantly, forecast accuracy is also linked to how closely the errors correlate with the actual values. RAE is a statistical measure used to assess the accuracy of predictive models with numerical data, common in regression and time series forecasting. RRSE is a statistical measure used to assess the accuracy of predictive models, especially in regression and time series forecasting (Wong et al. 2021).

$$RMSE = \sqrt{\frac{\sum_{t=1}^{T} (x_t - x_t\prime)^2}{T}} \tag{23}$$

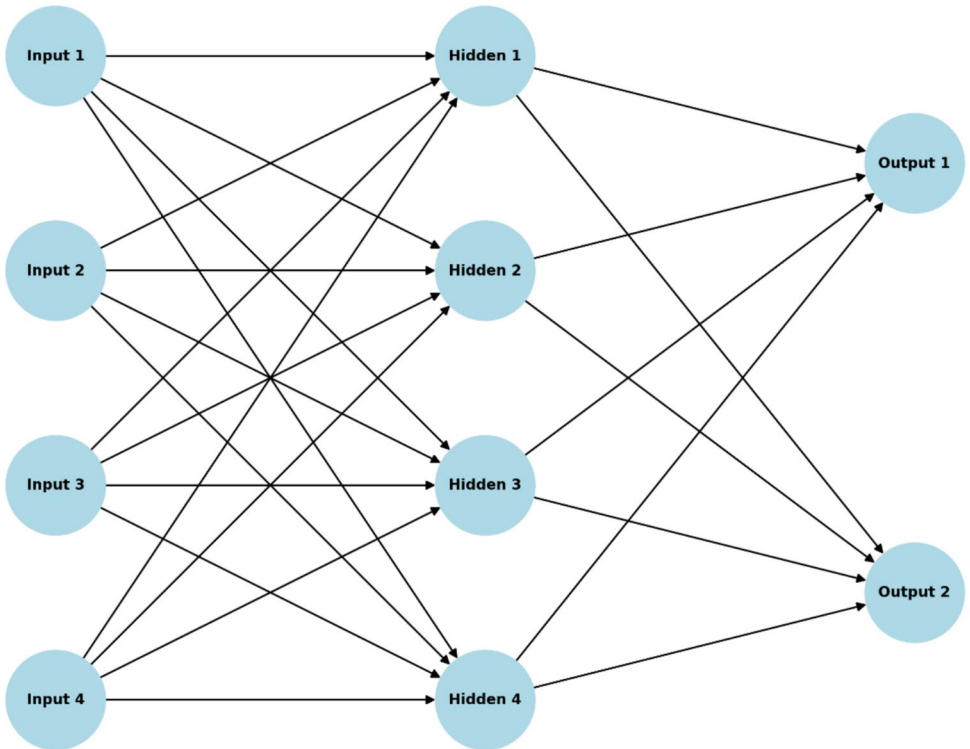

Fig. 3 The architecture of multilayer perception model

$$MAE = \frac{100}{T}\sum_{t=1}^{T}\left|\frac{x_t - x_t\prime}{x_t}\right| \quad (24)$$

$$RAE = \frac{\sum|x_t - x_t'|}{\sum|x_t - \dot{x}|} \quad (25)$$

$$RRSE = \sqrt{\frac{\sum\left(x_t - x_t'\right)^2}{\sum\left(x_t - \dot{x}\right)^2}} \quad (26)$$

Figure 4 shows a comprehensive framework for analyzing climate and drought conditions using both statistical and machine learning methods. It begins with the collection of monthly climate data—including precipitation, evapotranspiration, temperature, humidity, and streamflow—used to compute standardized drought indices such as SPI, SPEI, and SDI. Trend analysis is conducted through the MK, SS, and IPTA methods to identify statistically significant changes over time. Concurrently, SDI values are predicted using machine learning models including MLP, LR, SVM, and RF. These models are evaluated through performance comparisons to determine the most accurate prediction algorithm.

3 Study area

Diyarbakır province is located in southeastern Turkey (Fig. 5), covering an area of 15.272 km^2. Influenced by a continental climate, it experiences hot and dry summers and cold, rainy winters (Çelik 2015). The annual average temperature is 15.7 °C, with extreme temperatures ranging from a maximum of 45.2 °C to a minimum of-12.2 °C. The total annual precipitation is 496.25 mm, with

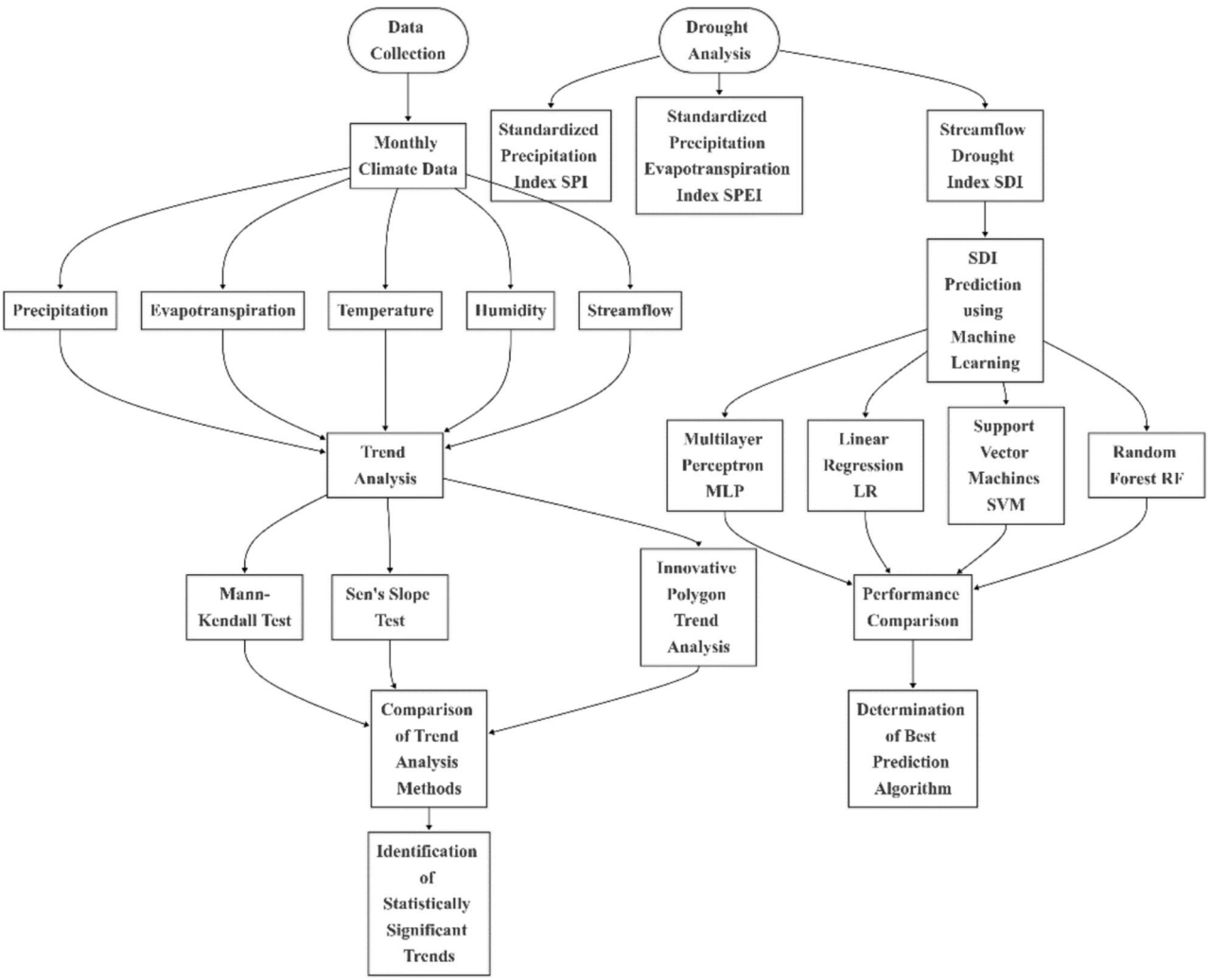

Fig. 4 A flowchart outlining the stages of data analysis and results in this study

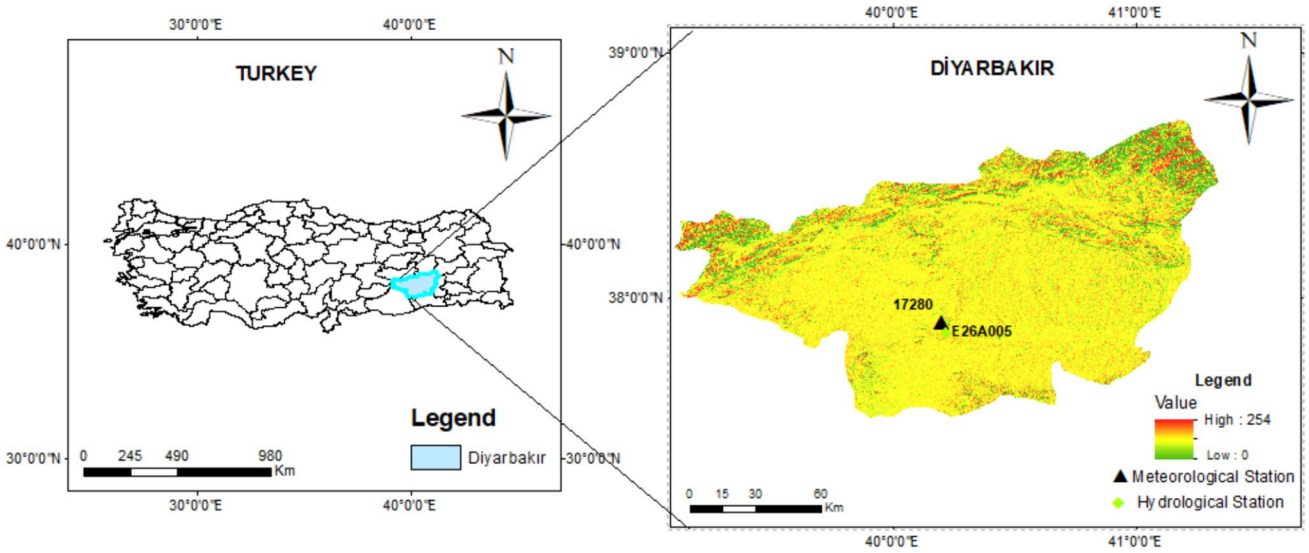

Fig. 5 The location of selected stations on the study area

rainfall concentrated mostly in the winter months, while drought conditions dominate the summer season (Çağlak and Türkeş 2023).

The Tigris River is the most important water source for Diyarbakır, playing a crucial role in irrigation and potable water supply. Additionally, structures such as the Hezan Dam and Çat Dam are vital for water resource management. Other water sources in the region, including ponds and streams primarily used for irrigation, are essential for agricultural activities (Varol et al. 2010).

Monthly data on precipitation, temperature, relative humidity, evaporation, and flow were obtained from the Turkish State Meteorological Service and the General Directorate of State Hydraulic Works. These data cover meteorological records from 1963 to 2021. Statistical analyses conducted on this data included calculations for mean, standard deviation, coefficient of variation (C_v), skewness coefficient (C_s), and first-order autocorrelation coefficient (r_1). These analyses provide significant insights into the climatic and hydrological conditions of Diyarbakır. The related data and statistical summaries are presented in Table 2.

4 Results

Trend analysis was applied to meteorological and hydrological variables in Diyarbakır at a 95% confidence level, and the results are presented in Fig. 6. For the precipitation variable, an increasing trend was observed only in June, while no significant trends were found in other months. In the temperature and evaporation variables, increasing trends were observed in June, August, and October, with no significant changes detected in the other months. The humidity variable showed a decreasing trend in June, July, August, and September. Analysis using Sen's slope method revealed the highest increasing trend in evaporation during June and August. For the flow variable, no significant trend was identified, though a decreasing tendency was observed, particularly in March, as well as in January, February, April, June, July, August, and September.

Table 2 Statistical analysis of climate data from Diyarbakır meteorological station

Station	Variables	Latitude	Longitude	Mean	SD	Cv	Cs	r_1
17,280	Precipitation (mm)	37.9	40.2	496.25	128.3	0.25	0.15	1.01
	Temperature (°C)			15.82	0.82	0.05	−0.42	0.99
	Evapotranspiration (mm)			940.65	51.12	0.05	−0.39	0.99
	Relative Humidity (%)			54.36	4.75	0.08	0.4	1
E26 A005	Streamflow (m^3/s)	37.8	40.22	67.33	24.67	0.36	1.04	1.02

Mean: annual total mean precipitation, *SD* standard deviation, *Cv* coefficient of variance, *Cs* skewness, r_1 kurtosis

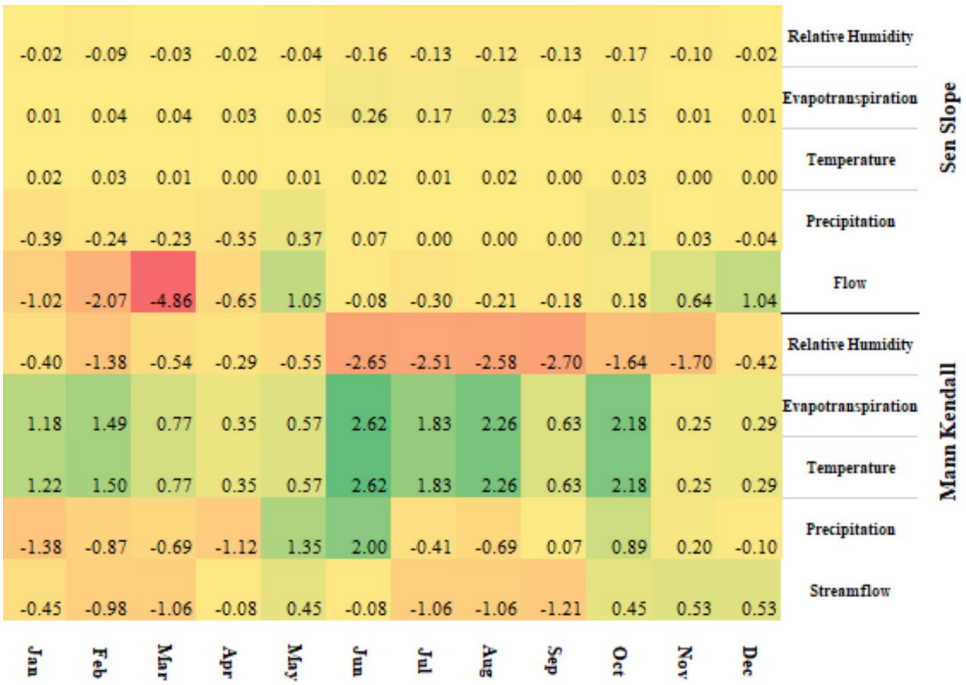

Fig. 6 Results of the MK and SS test for Diyarbakır Province

The results of the analysis conducted using the Innovative Polygon Trend Analysis (IPTA) method are presented in Fig. 7. According to the findings, the Mann–Kendall method identified a significant trend in the precipitation only in June, whereas the IPTA method revealed trends in all months except July and August. For temperature and evaporation variables, the MK method detected increasing trends in June, August, and October, but the IPTA method identified significant tendencies even in months where no trend was found with the traditional approach. In the case of humidity, both the MK and IPTA methods showed a decreasing trend in June, July, August, and September, with the IPTA method highlighting tendencies even in months without clear trends. For the flow variable, the MK method did not detect any significant trends throughout the year, whereas the IPTA method revealed increasing or decreasing tendencies in all months. These results demonstrate that the IPTA method provides higher accuracy in trend detection compared to the classical MK method.

Figure 8 indicates the trends of meteorological and hydrological variables in Diyarbakır province were examined using various methods, followed by drought analysis using the SPI and SPEI indices over 1-, 3-, 6-, 9-, 12-, and 24-month time scales. Additionally, for the more accurate 12- and 24-month periods, the time-based relationship of the SDI drought index with the SPI and SPEI indices was investigated. The corresponding time series are presented in Fig. 8. During the drought analysis, months with values below 0 were classified as drought periods, while months with values above 0 represented wet periods. The SPI index calculations used only monthly precipitation data, whereas the SDI index calculations were based solely on monthly flow data. For the SPEI index, both precipitation and temperature data were considered. Analysis of SPI and SPEI from 1961 to 2021 and SDI from 1980 to 1997 showed similar behavior across all three drought indices. The relationship between SDI and SPI/SPEI revealed that hydrological drought tends to follow meteorological drought. The SPI-12 and SPEI-12 show similar patterns but SPEI-12 may indicate slightly more severe drought conditions at times since it accounts for evapotranspiration. The SDI-12 sometimes lags behind the other indices, which is expected as hydrological drought often follows meteorological drought (measured by SPI/SPEI). When SDI-12 values are lower than SPI-12/SPEI-12, it suggests that streamflow response to precipitation deficits is more pronounced.

Figure 9 presents the correlations between the SPI and SPEI drought indices for Diyarbakır province. In short-term time scales (1–3 months), the correlation ranges between 61 and 74%. A particularly low correlation of 61% was observed at the 1-month time scale, indicating a weak relationship between SPI and SPEI in the short term. This low correlation is attributed to the inclusion of additional variables like temperature and evapotranspiration in the SPEI index. During periods of significant temperature fluctuations, the relationship between SPI and SPEI becomes weaker. At the 3-month time scale, the correlation increases to 74%, reflecting the stabilization of short-term precipitation and humidity deficits.

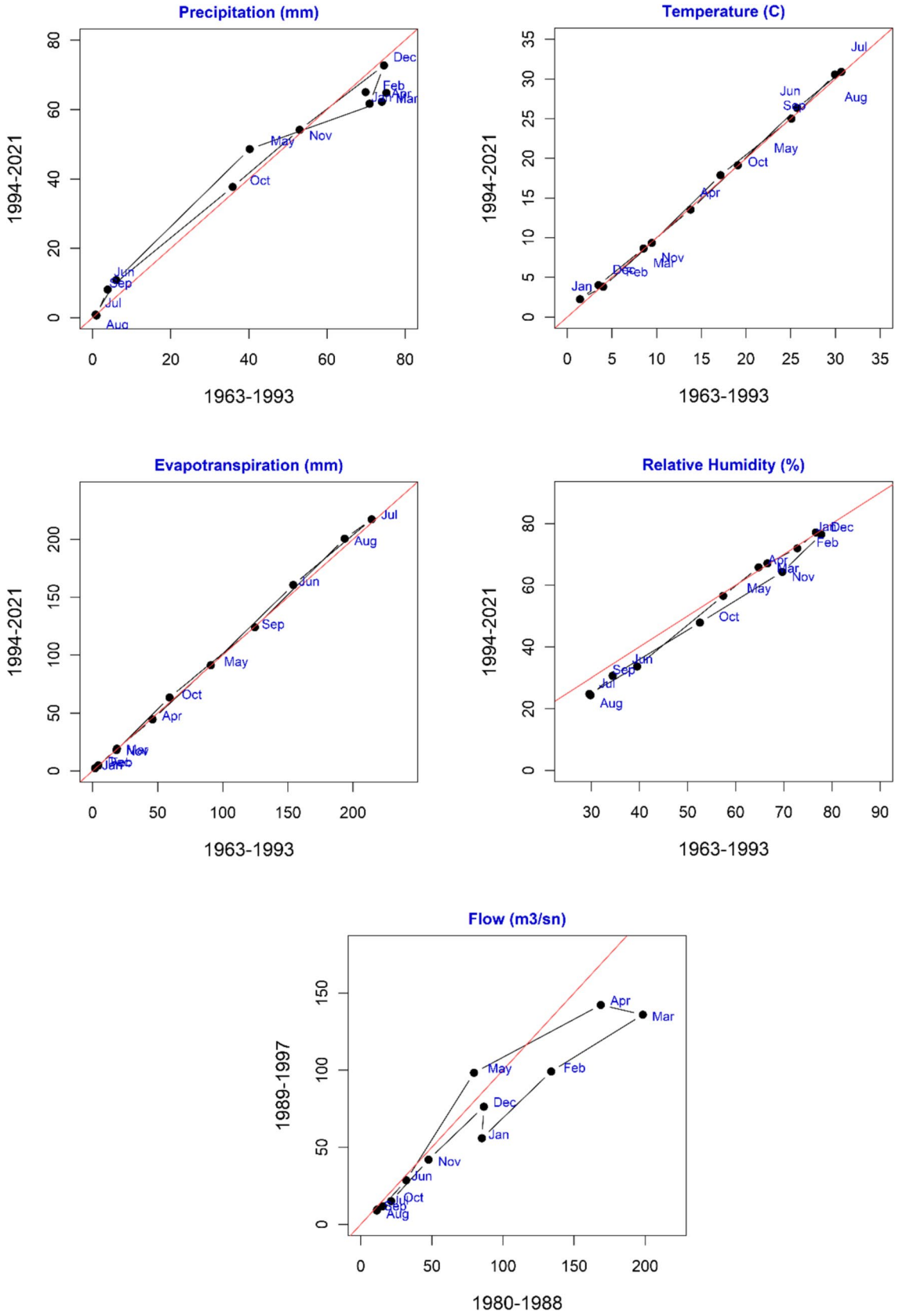

Fig. 7 Monthly trends of meteorological and hydrological variables according to the IPTA method

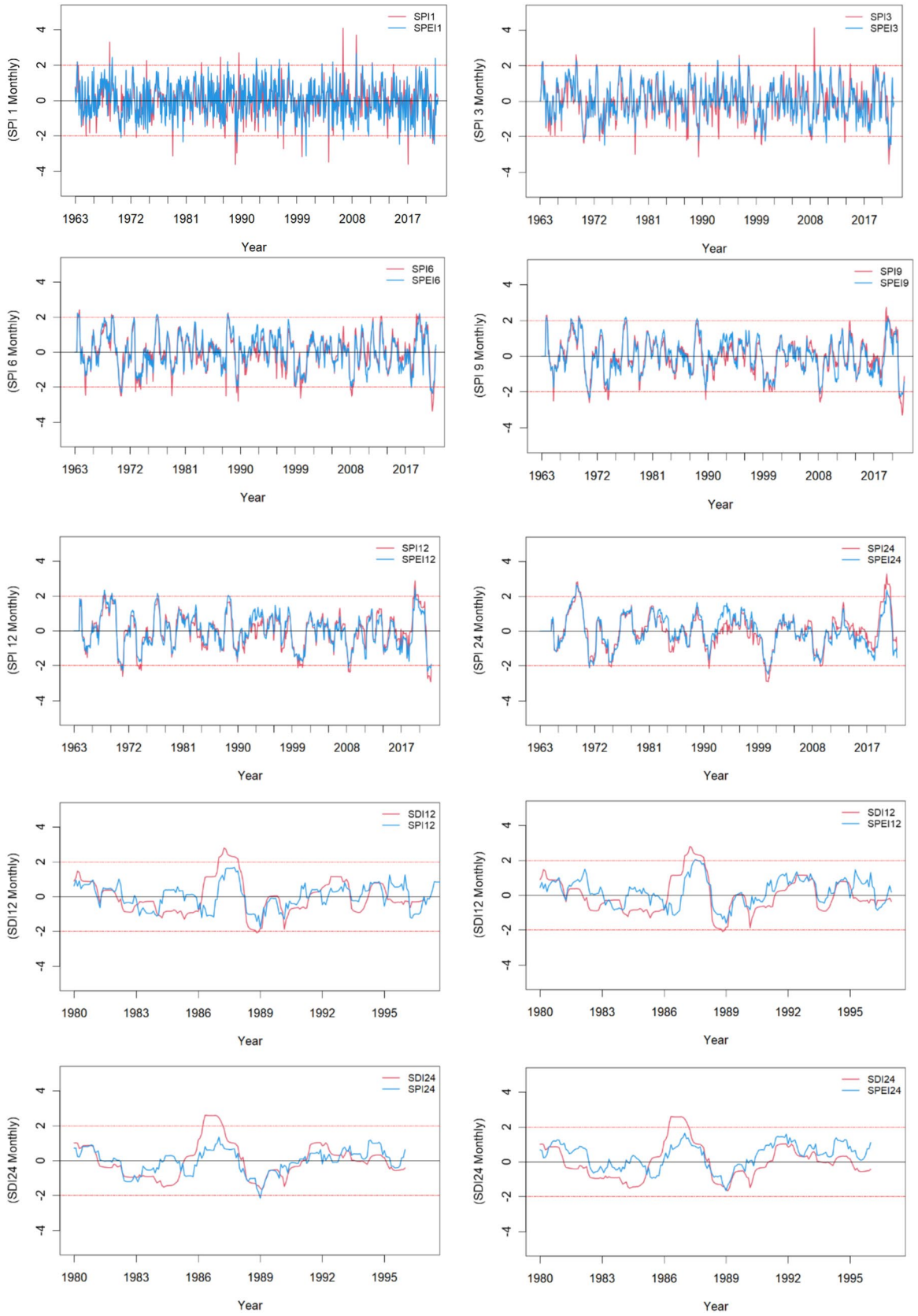

Fig. 8 Time series of drought indices at different time scales for Diyarbakır Province

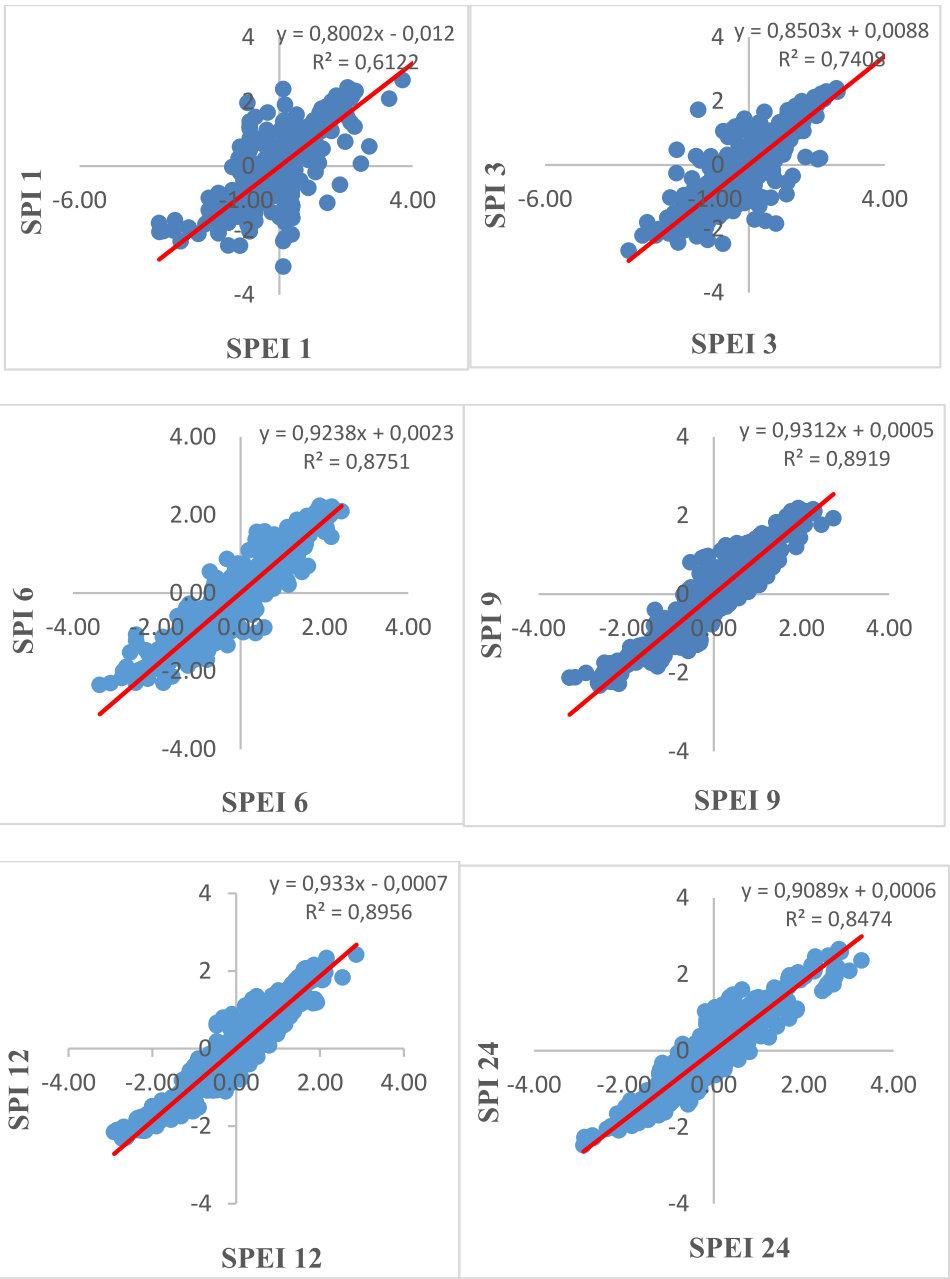

Fig. 9 Correlations between drought indices

In medium-term time scales (6–9–12 months), the correlation ranges between 87 and 90%. Specifically, a correlation of 87% was observed at the 6-month scale, 89% at the 9-month scale, and 90% at the 12-month scale, indicating the strongest relationship between SPI and SPEI during this period. The stronger correlation observed in the medium term is due to the balanced alignment of factors such as precipitation, temperature, and evapotranspiration.

In the long-term (24-month) time scale, the correlation decreases to 84%. Although the 12-month scale reaches a peak correlation of 90%, the 24-month period shows a decline to 84%. This reduction is attributed to the increasing impact of temperature over longer durations and the growing effects of evaporation losses on soil moisture and groundwater levels. Since SPI only considers precipitation data, while SPEI incorporates both precipitation and temperature data, the results differ more significantly over extended time scales.

The relationship between the SDI drought index and SPI and SPEI indices was also analyzed across similar time scales. In the 1- and 3-month time scales, the correlation ranged between 15 and 20%, while the 6-month time scale showed a correlation of approximately 30%. The correlation increased to 40% at the 9- and 12-month time scales and reached 45% at the 24-month scale. When examining the relationship between SPI, SPEI, and SDI,

Table 3 Number of drought occurrences across different time-scale drought indices

SPI						
	SPI 1	SPI 3	SPI 6	SPI 9	SPI 12	SPI 24
Mild drought	221	237	234	236	224	217
Moderate drought	49	62	51	47	54	65
Severe drought	26	24	31	30	27	28
Extreme drought	14	23	30	32	40	40
Non-Drought	398	362	362	363	363	358
SPEI						
	SPEI 1	SPEI 3	SPEI 6	SPEI 9	SPEI 12	SPEI 24
Mild drought	249	255	234	238	228	248
Moderate drought	70	69	70	61	64	55
Severe drought	28	28	34	37	37	44
Extreme drought	15	13	13	13	14	10
Non-Drought	346	341	352	351	354	328
SDI						
	SDI 1	SDI 3	SDI 6	SDI 9	SDI 12	SDI 24
Mild drought	79	83	87	92	97	75
Moderate drought	21	19	20	12	9	25
Severe drought	5	6	3	5	8	3
Extreme drought	6	6	5	5	2	0
Non-Drought	105	100	96	94	89	90

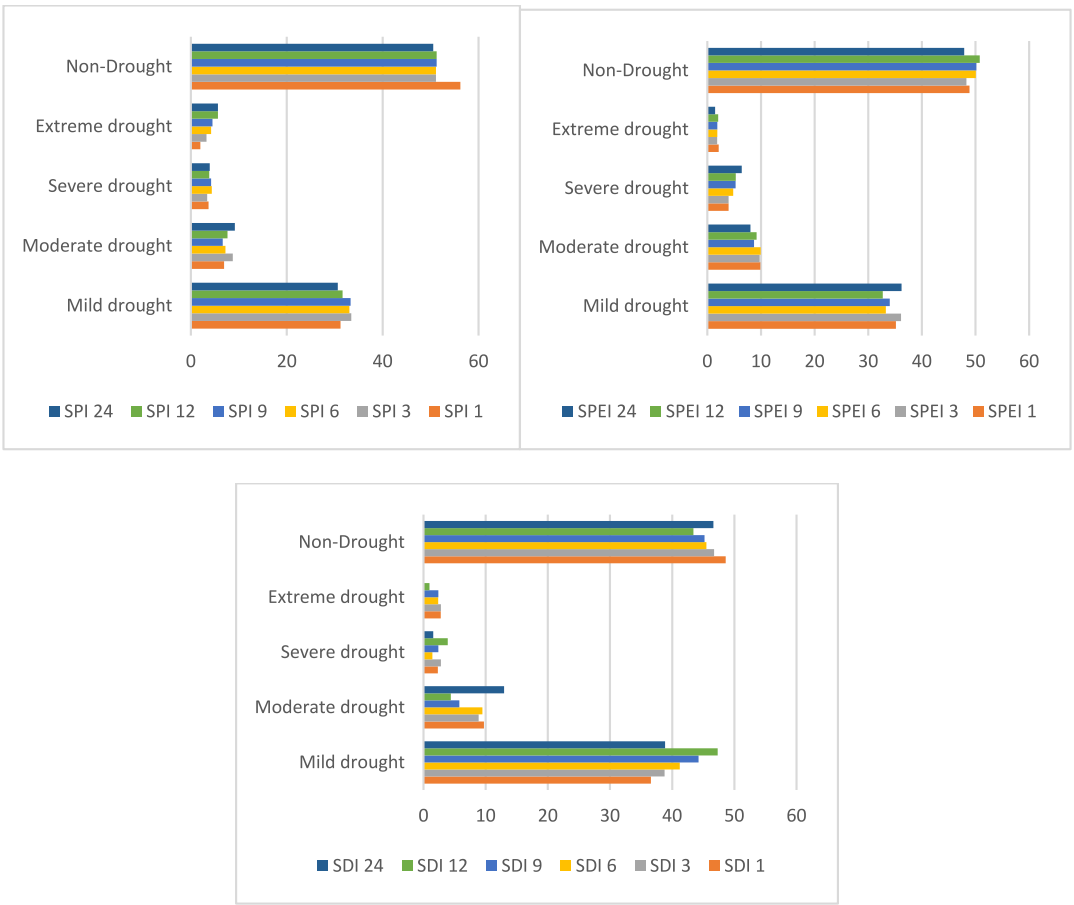

Fig. 10 Distribution of drought occurrences by different categories

the highest correlation of 35% was observed between SDI 3 and SPI 6–SPEI 6. No strong correlation was observed in other time intervals. These findings indicate that the relationship between SDI and SPI/SPEI varies depending on the time scale and that each index exhibits different relationships over varying periods.

The number of drought occurrences of varying severity in Diyarbakır is presented in Table 3 for SPI and SPEI and SDI. The percentage distribution of these occurrences is illustrated in Fig. 10. For the SPI drought index, mild drought is more common in the short term (1–3 months) and decreases as the time scale increases. The number of moderate droughts fluctuates over different time scales but generally remains stable. Severe droughts show little variation over time, with the highest occurrences observed at 6-month and 9-month time scales. Extreme drought tends to increase with longer time scales, reaching its peak levels at 12-month and 24-month scales. Non-drought periods are observed at high rates across all time scales.

For the SPEI drought index, mild drought is more prevalent in the short term but decreases over longer periods. Moderate droughts show a slight decrease as the time scale increases. Severe droughts increase over longer periods, reaching their highest levels at the 24-month time scale. Extreme drought is more frequent in the short term but shows a declining trend over time. Non-drought periods are generally observed at higher rates across all time scales.

For the SDI drought index, mild drought is common in the short term but shows a decreasing trend over time. Moderate droughts stabilize around the 6-month period but are observed at higher rates over the long term. Severe droughts are less frequent and typically occur at 12-month and 24-month time scales. Although extreme drought is more common in the short term, it is rarely observed over the long term. Non-drought periods are more frequently observed at 1- to 6-month time scales.

Finally, the explanatory power of the SDI index was investigated using methods such as Linear Regression (LR), Support Vector Machines (SVM), Random Forest (RF), and Multilayer Perceptron (MLP), where SPI and SPEI indices at different time scales were treated as dependent variables, and the SDI index was treated as the independent variable. The results obtained from this analysis are presented in Table 4.

Different methods were used to predict the SDI drought index, with the highest R^2 value achieved using the Random Forest algorithm. The model's dataset consisted of 193 samples and included three variables: SDI 24, SPI 24, and SPEI 24. A tenfold cross-validation technique was employed to evaluate the model's performance. The Random Forest algorithm was implemented as an ensemble model composed of 100 decision trees. Model performance was assessed using the following metrics: correlation coefficient, Mean Absolute Error (MAE), Root Mean Squared Error (RMSE), Relative Absolute Error (RAE), and Root Relative Squared Error (RRSE). The results demonstrated that the Random Forest model is a reliable and effective tool for predicting the SDI drought index.

The R^2 value represents the linear relationship between the predicted and actual values. A high value of 0.8322 indicates a strong correlation established by the model.

Mean Absolute Error (MAE): MAE measures the average deviation of the model's predictions from the actual values. The model's average prediction error was approximately 0.36 units. Lower MAE values indicate better predictive performance.

Root Mean Squared Error (RMSE): RMSE is calculated by taking the square root of the average squared errors. Since it penalizes larger errors more heavily, RMSE values are generally higher than MAE. An RMSE value of 0.5547 shows that the model maintains a relatively low error level.

Relative Absolute Error (RAE): RAE expresses the model's MAE as a percentage relative to a simple average model. The model outperforms the average model by approximately 55%. Lower RAE values indicate better model performance.

Table 4 Data results of the models used in the study

Model		LR	SVM	RF	MLP
SDI 1 = SPI 1 + SPEI 1	R2	0.35	0.30	0.19	0.2
	MAE	0.75	0.76	0.84	0.79
	RMSE	0.93	0.95	1	1
	RAE	93.4	95	105	99
	RRSE	92.9	94	104	101
SDI 3 = SPI 3 + SPEI 3	R2	0.48	0.48	0.33	0.41
	MAE	0.71	0.72	0.82	0.75
	RMSE	0.87	0.87	1	0.94
	RAE	90	90	103	94
	RRSE	86	87	100	93
SDI 6 = SPI 6 + SPEI 6	R2	0.59	0.58	0.62	0.49
	MAE	0.65	0.67	0.64	0.7
	RMSE	0.8	0.82	0.8	0.8
	RAE	82	84	81	88
	RRSE	80	81	80	88
SDI 9 = SPI9 + SPEI 9	R2	0.61	0.61	0.58	0.52
	MAE	0.63	0.63	0.65	0.69
	RMSE	0.78	0.8	0.83	0.87
	RAE	79	79	80	85
	RRSE	78	79	82	87
SDI 12 = SPI 12 + SPEI 12	R2	0.63	0.63	0.67	0.58
	MAE	0.61	0.61	0.54	0.66
	RMSE	0.77	0.78	0.74	0.83
	RAE	76	76	67	81
	RRSE	76	77	74	83
SDI 24 = SPI 24 + SPEI 24	R2	0.67	0.67	**0.83**	0.58
	MAE	0.55	0.54	**0.35**	0.7
	RMSE	0.73	0.74	**0.55**	0.8
	RAE	69	68	**44**	88
	RRSE	73	74	**55**	87

Root Relative Squared Error (RRSE): This metric uses RMSE to express the model's error rate relative to the standard deviation of the dataset. The model's error rate corresponds to 55.30% of the dataset's variability. Lower RRSE values reflect better model performance.

The error graphs obtained from the models used in the study are presented in Fig. 11. When examining the error graphs in the article, the differences in the prediction performance of the machine learning algorithms used become clearly evident. The Random Forest (RF) algorithm demonstrated the best performance with low Mean Absolute Error (MAE) and Root Mean Squared Error (RMSE) values. The low error rates of the RF model indicate its ability to successfully capture patterns in the dataset and accurately model the relationships between complex climate variables.

On the other hand, higher error values were observed in the Linear Regression (LR) and Support Vector Machines (SVM) models. This can be attributed to the insufficient flexibility of these algorithms, particularly with high-dimensional and non-linear data. Although the Multilayer Perceptron (MLP) model is capable of recognizing non-linear relationships, it faced some challenges in adequately generalizing the dataset, reflected in its higher error values.

Based on these error graphs, it can be concluded that the RF algorithm is the most reliable method for predictions involving climate data and should be the preferred model for drought forecasting related to climate change. Additionally, analyzing the error graphs of different models provides valuable insights for model selection and optimization processes.

Figure 12 provides a detailed comparison of four machine learning models (LR, MLP, RF, and SVM) with actual data using four distinct visualization methods. Looking at the top left, the Taylor diagram shows how well each model correlates with observed data. The MLP (Multi-Layer Perceptron) appears to have the highest correlation (closest to the"Observed"point on the x-axis), followed by RF (Random Forest), while LR (Linear Regression) and SVM (Support Vector Machine) show lower correlations. The violin plot (top right) reveals the distribution of values across models. The actual data (red) shows a peaked distribution with some outliers at both ends. The RF model (blue) most closely matches the actual data's shape and range, while SVM (purple) has a narrower distribution, suggesting it might be underfitting some extreme values. The CDF plot (bottom left) confirms this pattern—the SVM line (purple) diverges most from the actual data line (red), particularly at the lower end of values. The RF and MLP models track the actual data CDF more closely throughout the distribution. Finally, the PDF plot (bottom right) shows density distributions. The RF model appears to best capture the actual data's slight right skew and overall shape, though it might slightly underestimate the peak density around zero.

Overall, the Random Forest (RF) model seems to be performing best at capturing the distribution characteristics of the actual data, with MLP showing strong correlation but perhaps not matching the full distribution as well. The SVM

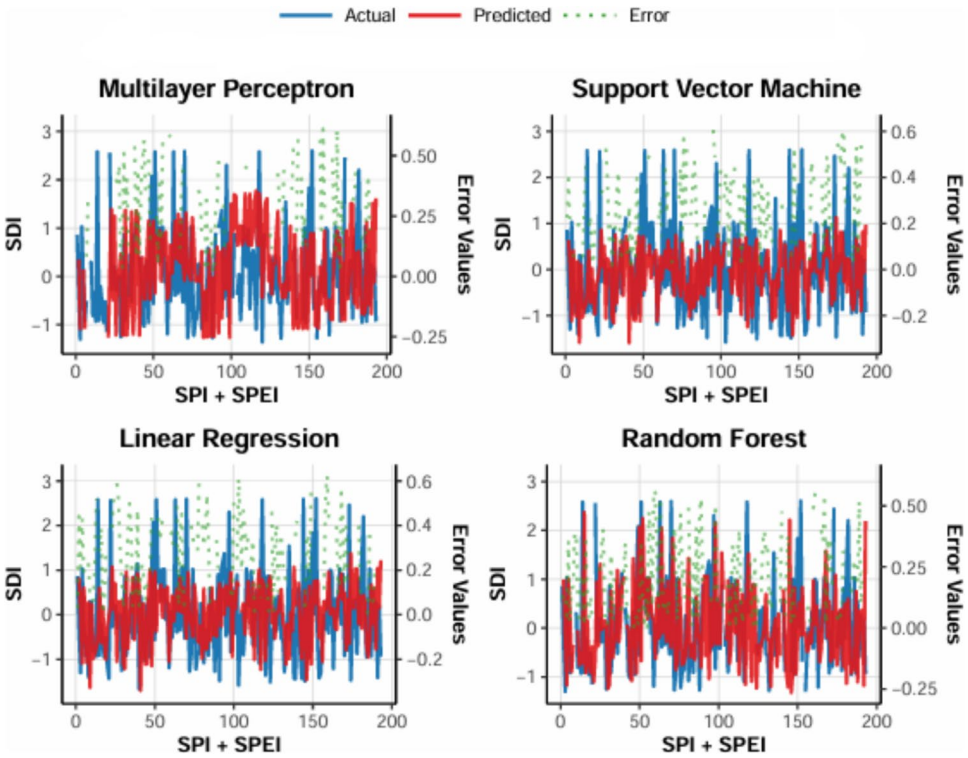

Fig. 11 Comparison of actual and predicted values with error distribution

model appears to be the weakest performer, particularly at capturing the extremes of the distribution.

5 Conclusion

This study comprehensively analyzes the impacts of climate change on hydrological and meteorological variables in Diyarbakır. Traditional and innovative trend analysis methods, including the MK, SS, and the IPTA, were employed to examine long-term changes in precipitation, temperature, humidity, evaporation, and flow data. The findings demonstrate the superior trend detection capacity of the IPTA method compared to classical methods.

The comparative analysis between the Mann–Kendall (MK) and Innovative Polygon Trend Analysis (IPTA) methods reveals that IPTA demonstrates superior sensitivity in detecting climate variable trends. While the MK

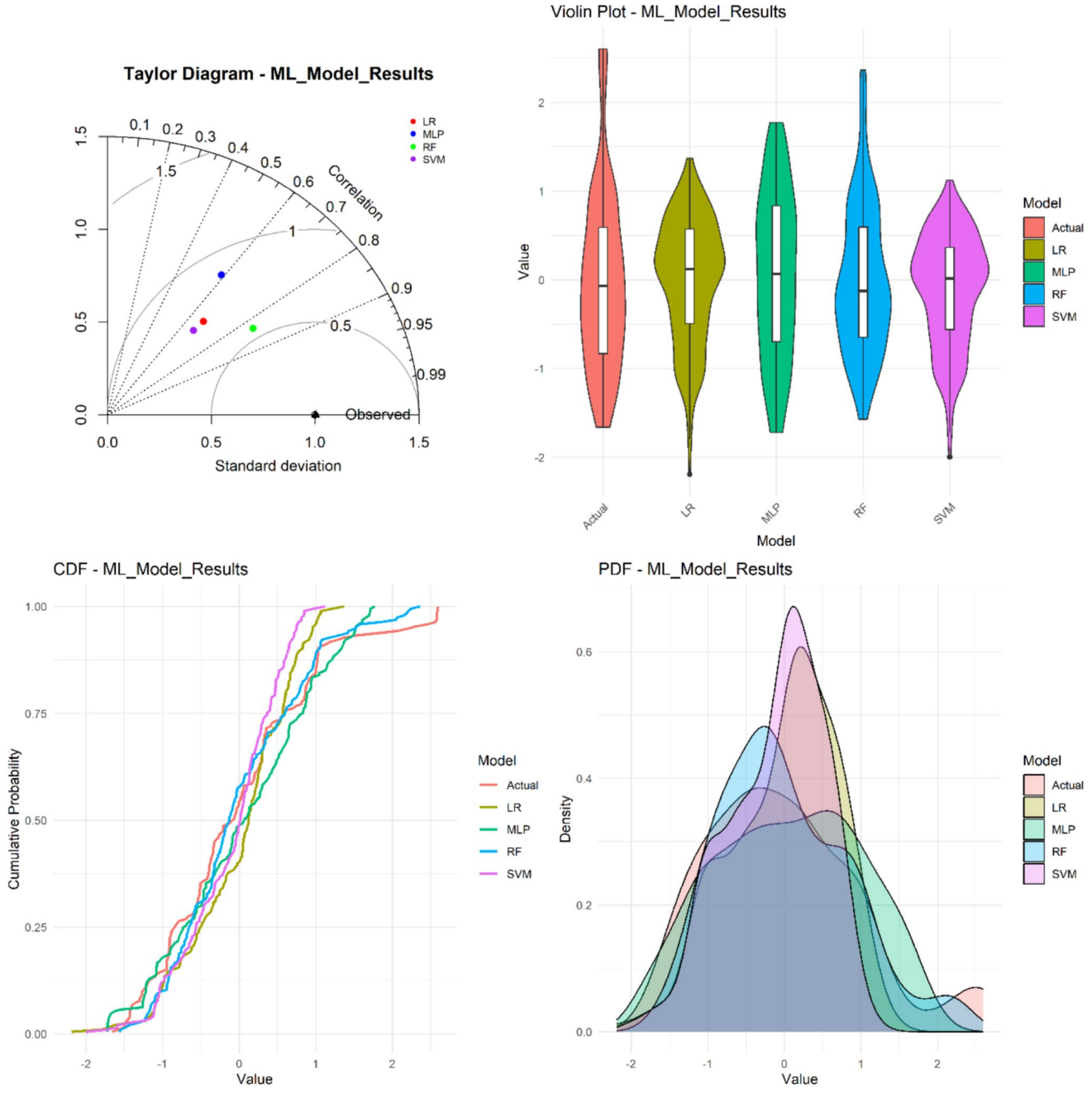

Fig. 12 A comprehensive comparison of four machine learning models (LR, MLP, RF, and SVM) against actual data through four different visualization techniques

method identified limited significant trends across the analyzed parameters (precipitation, temperature, evaporation, humidity, and flow), IPTA consistently detected meaningful tendencies in most months for all variables. Our results are convenient with the literatures (Robleh et al. 2024; Berhail and Katipoğlu 2024; Gul et al. 2025; Yuce et al. 2025).

For drought analysis, various indices such as the SPI, SPEI, and SDI were used. Analyses conducted across 1-, 3-, 6-, 9-, 12-, and 24-month time scales revealed variations in drought trends over different periods. Stronger correlations between SPI, SPEI, and SDI were observed, particularly over long-term time scales. In Diyarbakır, short-term mild droughts are common across all indices, while long-term extreme droughts are more prevalent for SPI. Moderate droughts show varied trends depending on the index and timescale. Non-drought periods are generally frequent across all indices and timescales.

In machine learning-based analyses, SDI was predicted using MLP, LR, SVM, and RF algorithms. The study concluded that the Random Forest algorithm, utilizing SDI 24, SPI 24, and SPEI 24 as input variables and evaluated through tenfold cross-validation, demonstrated the highest accuracy ($R^2 = 0.8322$ and low error metrics) in predicting the SDI drought index compared to Linear Regression, Support Vector Machines, and Multilayer Perceptron models, making it the preferred method for climate-related drought forecasting.

In conclusion, this study provides a comprehensive assessment of climate change impacts in Diyarbakır, highlighting the effectiveness of both traditional trend analysis methods and machine learning algorithms. The findings offer valuable data for the sustainable management of water resources and drought risk reduction in the region. The high accuracy provided by machine learning algorithms paves the way for more widespread use of these techniques in future studies. These results serve as a guide for policymakers in developing local and national water management policies, climate adaptation strategies, and risk management plans.

Acknowledgements Acknowledgments are due to state water Works (DSI), general directorate of meteorology (MGM) for providing meteorological data

Author contribution Musa Esit: data gathering, hydrometeorological data trend analysis, interpretation of the findings, manuscript writing, and submission. Recep Celik: supervision and editing. Ergun Akbas: material preparation, data collection, and analysis, Ibrahim Halil Deger: interpretation of the revised analysis.

Funding Not applicable.

Data availability No datasets were generated or analysed during the current study.

Code availability Not applicable.

Declarations

Ethics approvals Not applicable.

Consent to participate Not applicable.

Consent for publication Not applicable.

Informed consent This study did not include any human participants or animals.

Competing interest The authors declare no competing interests.

References

Abro MI, Elahi E, Chand R et al (2022) Estimation of a trend of meteorological and hydrological drought over Qinhuai River Basin. Theor Appl Climatol 147:1065–1078. https://doi.org/10.1007/s00704-021-03870-z

Achite M, Ceribasi G, Ceyhunlu AI et al (2021) The Innovative Polygon Trend Analysis (IPTA) as a Simple Qualitative Method to Detect Changes in Environment—Example Detecting Trends of the Total Monthly Precipitation in Semiarid Area. Sustainability 13:12674. https://doi.org/10.3390/su132212674

Achite M, Jehanzaib M, Elshaboury N, Kim T-W (2022) Evaluation of Machine Learning Techniques for Hydrological Drought Modeling: A Case Study of the Wadi Ouahrane Basin in Algeria. Water 14:431. https://doi.org/10.3390/w14030431

Adarsh S, Karthik S, Shyma M et al (2018) Developing Short Term Drought Severity-Duration-Frequency Curves for Kerala Meteorological Subdivision, India Using Bivariate Copulas. KSCE J Civ Eng 22:962–973. https://doi.org/10.1007/s12205-018-1404-9

AghaKouchak A, Pan B, Mazdiyasni O et al (2022) Status and prospects for drought forecasting: opportunities in artificial intelligence and hybrid physical–statistical forecasting. Philosophical Transactions of the Royal Society a: Mathematical, Physical and Engineering Sciences 380:20210288. https://doi.org/10.1098/rsta.2021.0288

Aghelpour P, Varshavian V (2021) Forecasting Different Types of Droughts Simultaneously Using Multivariate Standardized Precipitation Index (MSPI), MLP Neural Network, and Imperialistic Competitive Algorithm (ICA). Complexity 2021:6610228. https://doi.org/10.1155/2021/6610228

Aghelpour P, Bahrami-Pichaghchi H, Varshavian V (2021) Hydrological drought forecasting using multi-scalar streamflow drought index, stochastic models and machine learning approaches, in northern Iran. Stoch Environ Res Risk Assess 35:1615–1635. https://doi.org/10.1007/s00477-020-01949-z

Akbari H, Rakhshandehroo GR, Sharifloo AH, Ostadzadeh E (2015) Drought analysis based on Standardized Precipitation Index (SPI) and Streamflow Drought Index (SDI) in Chenar Rahdar River Basin, Southern Iran. 11–22. https://doi.org/10.1061/9780784479322.002

Aksoy H, Cavus Y (2022) Discussion of "Drought assessment in a south Mediterranean transboundary catchment." Hydrol Sci J 67:150–156. https://doi.org/10.1080/02626667.2021.2009838

Alahacoon N, Edirisinghe M (2022) A comprehensive assessment of remote sensing and traditional based drought monitoring indices at global and regional scale. Geomat Nat Haz Risk 13:762–799. https://doi.org/10.1080/19475705.2022.2044394

Alkan A, Tombul M (2024) Drought Forecasting of Seyhan and Ceyhan Basins Using Machine Learning Methods. Water Resour 51:12–26. https://doi.org/10.1134/S0097807823600973

Alkubaisi H, Mehr AD, A S, Khan MMH (2024) Drought modelling and forecasting using shallow and deep machine learning techniques. Model Earth Syst Environ 11:41. https://doi.org/10.1007/s40808-024-02268-w

Ashraf MS, Ahmad I, Khan NM et al (2021) Streamflow Variations in Monthly, Seasonal, Annual and Extreme Values Using Mann-Kendall, Spearmen's Rho and Innovative Trend Analysis. Water Resour Manage 35:243–261. https://doi.org/10.1007/s11269-020-02723-0

Avsaroglu Y, Gumus V (2022) Assessment of hydrological drought return periods with bivariate copulas in the Tigris river basin. Turkey Meteorol Atmos Phys 134:95. https://doi.org/10.1007/s00703-022-00933-2

Ayugi B, Eresanya EO, Onyango AO et al (2022) Review of Meteorological Drought in Africa: Historical Trends, Impacts, Mitigation Measures, and Prospects. Pure Appl Geophys 179:1365–1386. https://doi.org/10.1007/s00024-022-02988-z

Belayneh A, Adamowski J, Khalil B (2016) Short-term SPI drought forecasting in the Awash River Basin in Ethiopia using wavelet transforms and machine learning methods. Sustain Water Resour Manag 2:87–101. https://doi.org/10.1007/s40899-015-0040-5

Bellprat O, Guemas V, Doblas-Reyes F, Donat MG (2019) Towards reliable extreme weather and climate event attribution. Nat Commun 10:1732. https://doi.org/10.1038/s41467-019-09729-2

Bera D, Dutta D (2024) Analysing spatio-temporal drought characteristics and copula-based return period in Indian Gangetic Basin (1901–2021). Environ Sci Pollut Res 31:22471–22493. https://doi.org/10.1007/s11356-024-32286-1

Berhail S, Katipoğlu OM (2024) Exploring hydrological and meteorological drought trends in Northeast Algeria: implications for water resource management. Theor Appl Climatol 155:9689–9712. https://doi.org/10.1007/s00704-024-05207-y

Boudiaf B, Şen Z, Boutaghane H (2022) North coast Algerian rainfall monthly trend analysis using innovative polygon trend analysis (IPTA). Arab J Geosci 15:1626. https://doi.org/10.1007/s12517-022-10907-8

Breiman L (2001) Random Forests. Mach Learn 45:5–32. https://doi.org/10.1023/A:1010933404324

Çağlak S, Türkeş M (2023) Spatial Distribution and Future Projections of Thermal Comfort Conditions during the Hot Period of the Year in Diyarbakır City. Southeastern Turkey Sustainability 15:10473. https://doi.org/10.3390/su151310473

Cancelliere A, Mauro GD, Bonaccorso B, Rossi G (2007) Drought forecasting using the Standardized Precipitation Index. Water Resour Manage 21:801–819. https://doi.org/10.1007/s11269-006-9062-y

Çelik R (2015) Mapping of groundwater potential zones in the Diyarbakır city center using GIS. Arab J Geosci 8:4279–4286. https://doi.org/10.1007/s12517-014-1485-9

Ceribasi G, Ceyhunlu AI, Ahmed N (2021) Analysis of temperature data by using innovative polygon trend analysis and trend polygon star concept methods: a case study for Susurluk Basin, Turkey. Acta Geophys 69:1949–1961. https://doi.org/10.1007/s11600-021-00632-3

Dabanlı İ, Şen Z, Yeleğen MÖ et al (2016) Trend Assessment by the Innovative-Şen Method. Water Resour Manage 30:5193–5203. https://doi.org/10.1007/s11269-016-1478-4

Danandeh Mehr A, Sorman AU, Kahya E, Hesami Afshar M (2020) Climate change impacts on meteorological drought using SPI and SPEI: case study of Ankara, Turkey. Hydrol Sci J 65:254–268. https://doi.org/10.1080/02626667.2019.1691218

Dubrovsky M, Svoboda MD, Trnka M et al (2009) Application of relative drought indices in assessing climate-change impacts on drought conditions in Czechia. Theor Appl Climatol 96:155–171. https://doi.org/10.1007/s00704-008-0020-x

Durbach I, Merven B, McCall B (2017) Expert elicitation of autocorrelated time series with application to e3 (energy-environment-economic) forecasting models. Environ Model Softw 88:93–105. https://doi.org/10.1016/j.envsoft.2016.11.007

Elbeltagi A, Pande CB, Kumar M et al (2023) Prediction of meteorological drought and standardized precipitation index based on the random forest (RF), random tree (RT), and Gaussian process regression (GPR) models. Environ Sci Pollut Res 30:43183–43202. https://doi.org/10.1007/s11356-023-25221-3

Elbeltagi A, Srivastava A, Ehsan M et al (2024) Advanced stacked integration method for forecasting long-term drought severity: CNN with machine learning models. Journal of Hydrology: Regional Studies 53:101759. https://doi.org/10.1016/j.ejrh.2024.101759

Esit M (2022) Investigation of innovative trend approaches (ITA with significance test and IPTA) comparing to the classical trend method of monthly and annual hydrometeorological variables: a case study of Ankara region, Turkey. J Water Clim Chang jwc2022356. https://doi.org/10.2166/wcc.2022.356

Esit M, Çelik R, Akbas E (2023) Spatial and temporal variation of meteorological parameters in the lower Tigris-Euphrates basin, Türkiye: application of non-parametric methods and an innovative trend approach. Water Sci Technol 87:1982–2004. https://doi.org/10.2166/wst.2023.116

Esit M, Kumar S, Pandey A et al (2021) Seasonal to multi-year soil moisture drought forecasting. npj Clim Atmos Sci 4:1–8. https://doi.org/10.1038/s41612-021-00172-z

Firdaus T, Gupta P, Sangita Mishra S (2023) Implementing Machine Learning Models for Drought Prediction Based on Metrological Drought Indices with Varying Time Scales: A Case of Latur Region. In: Reddy KR, Kalia S, Tangellapalli S, Prakash D (eds) Recent Advances in Sustainable Environment. Springer Nature, Singapore, pp 183–195

Gaddikeri V, Sarangi A, Singh DK et al (2024) Trend and change-point analyses of meteorological variables using Mann-Kendall family tests and innovative trend assessment techniques in New Bhupania command (India). Journal of Water and Climate Change 15:2033–2058. https://doi.org/10.2166/wcc.2024.462

Gul S, Cui X, Ceribasi G et al (2025) Investigation of variability in monthly minimum and maximum temperature with trend methods in Khyber Pakhtunkhwa. Pakistan Ain Shams Engineering Journal 16:103296. https://doi.org/10.1016/j.asej.2025.103296

Helsel DR, Hirsch RM (2002) Statistical methods in water resources. U.S. Geological Survey, Reston, VA

IPCC (2013a) Climate change 2013: the physical science basis. Contribution of Working Group I to the Fifth Assessment Report of the Intergovernmental Panel on Climate Change [Stocker TFD, Qin GK, Plattner M, Tignor SK, Allen J, Boschung A, Nauels Y, Xia V, Bex ve PM, Midgley (eds.)]. Cambridge, UK: Cambridge University Press, 1535

Intergovernmental Panel on Climate Change (2013b) Climate Change 2013—the physical science basis (Fifth Assessment Report, Working Group I contribution). Headline Statements from the Summary for Policymakers. IPCC, Geneva

IPCC (2014) Climate Change 2014: Impacts, Adaptation, and Vulnerability. Part A: Global and Sectoral Aspects. — European Environment Agency. https://www.eea.europa.eu/data-and-maps/indicators/heating-degree-days-2/ipcc-2007-contribution-of-working. Accessed 11 Aug 2022

Jahangir MH, Yarahmadi Y (2020) Hydrological drought analyzing and monitoring by using Streamflow Drought Index (SDI) (case study: Lorestan, Iran). Arab J Geosci 13:110. https://doi.org/10.1007/s12517-020-5059-8

Jehanzaib M, Bilal Idrees M, Kim D, Kim T-W (2021) Comprehensive Evaluation of Machine Learning Techniques

for Hydrological Drought Forecasting. J Irrig Drain Eng 147:04021022. https://doi.org/10.1061/(ASCE)IR.1943-4774.0001575

Karbasi M, Jamei M, Malik A et al (2023) Multi-steps drought forecasting in arid and humid climate environments: Development of integrative machine learning model. Agric Water Manag 281:108210. https://doi.org/10.1016/j.agwat.2023.108210

Kartal V, Emiroglu ME (2024) Hydrological Drought and Trend Analysis in Kızılırmak, Yeşilırmak and Sakarya Basins. Pure Appl Geophys 181:1919–1943. https://doi.org/10.1007/s00024-024-03499-9

Katherine C, Dipak D, Gerhard K et al (2023) IPCC, 2023: Climate change 2023: Synthesis report. Contribution of working groups I, II and III to the sixth assessment report of the intergovernmental panel on climate change [Core Writing Team, H. Lee and J. Romero (eds.)]. IPCC, Geneva, Switzerland. https://doi.org/10.59327/ipcc/ar6-9789291691647

Kendall MG (1975) Rank correlation methods. Griffin, London

Kesgin E, Yaldız SG, Güçlü YS (2024) Spatiotemporal variability and trends of droughts in the Mediterranean coastal region of Türkiye. Int J Climatol 44:1036–1057. https://doi.org/10.1002/joc.8370

Koycegiz C, Buyukyildiz M (2024) Applications of innovative polygon trend analysis (IPTA) and trend polygon star concept (TPSC) methods for the variability of precipitation in Konya Closed Basin (Turkey). Theor Appl Climatol 155:2641–2656. https://doi.org/10.1007/s00704-023-04765-x

Kumar V, Sharma KV, Pham QB et al (2024) Advancements in drought using remote sensing: assessing progress, overcoming challenges, and exploring future opportunities. Theor Appl Climatol 155:4251–4288. https://doi.org/10.1007/s00704-024-04914-w

Kundu A, Dutta D, Patel NR, Denis DM (2024) Drought Dynamics: Enhanced Characterization Through Hyper-Temporal Satellite Observations. Hydrol Process 38:e70015. https://doi.org/10.1002/hyp.70015

Latifoğlu L, Bayram S, Aktürk G, Citakoglu H (2024) Drought index time series forecasting via three-in-one machine learning concept for the Euphrates basin. Earth Sci Inform 17:5841–5898. https://doi.org/10.1007/s12145-024-01471-8

Lotfirad M, Esmaeili-Gisavandani H, Adib A (2021) Drought monitoring and prediction using SPI, SPEI, and random forest model in various climates of Iran. Journal of Water and Climate Change 13:383–406. https://doi.org/10.2166/wcc.2021.287

Mann HB (1945) Nonparametric Tests Against Trend. Econometrica 13:245–259. https://doi.org/10.2307/1907187

McKee TB, Doesken NJ, Kleist J (1993) The Relationship of Drought Frequency and Duration to Time Scales. Boston, MA: American Meteorological Society 17:179–183

Mohseni Saravi M, Safdari AA, Malekian A (2009) Intensity-Duration-Frequency and spatial analysis of droughts using the Standardized Precipitation Index. Hydrology and Earth System Sciences Discussions 6:1347–1383. https://doi.org/10.5194/hessd-6-1347-2009

Mokhtarzad M, Eskandari F, Jamshidi Vanjani N, Arabasadi A (2017) Drought forecasting by ANN, ANFIS, and SVM and comparison of the models. Environ Earth Sci 76:729. https://doi.org/10.1007/s12665-017-7064-0

Nalbantis I (2008) Evaluation of a hydrological drought index. Eur Water 23.24(2008):67–77

Nalbantis I, Tsakiris G (2009) Assessment of Hydrological Drought Revisited. Water Resour Manage 23:881–897. https://doi.org/10.1007/s11269-008-9305-1

Oruc S, Hinis MA, Tugrul T (2024) Evaluating Performances of LSTM, SVM, GPR, and RF for Drought Prediction in Norway: A Wavelet Decomposition Approach on Regional Forecasting. Water 16:3465. https://doi.org/10.3390/w16233465

Özbeyaz A, Söylemez M (2020) Modeling compaction parameters using support vector and decision treeregression algorithms. Turk J Electr Eng Comput Sci 28:3079–3093. https://doi.org/10.3906/elk-1905-179

Pande CB, Sidek LM, Varade AM et al (2024) Forecasting of meteorological drought using ensemble and machine learning models. Environ Sci Eur 36:160. https://doi.org/10.1186/s12302-024-00975-w

Pei Z, Fang S, Wang L, Yang W (2020) Comparative Analysis of Drought Indicated by the SPI and SPEI at Various Timescales in Inner Mongolia. China Water 12:1925. https://doi.org/10.3390/w12071925

Prabowo MA, Soekirno S, Ananda N et al (2024) Drought prediction based standardized precipitation index using multilayer perceptron model. In: 2024 International conference on Smart Computing, IoT and Machine Learning (SIML) (pp 262–267). IEEE

Prodhan FA, Zhang J, Hasan SS et al (2022) A review of machine learning methods for drought hazard monitoring and forecasting: Current research trends, challenges, and future research directions. Environ Model Softw 149:105327. https://doi.org/10.1016/j.envsoft.2022.105327

Qadem Z, Tayfur G (2024) In-depth Exploration of Temperature Trends in Morocco: Combining Traditional Methods of Mann Kendall with Innovative ITA and IPTA Approaches. Pure Appl Geophys 181:2717–2739. https://doi.org/10.1007/s00024-024-03535-8

Robleh HB, Yuce MI, Esit M, Deger IH (2024) Meteorological drought monitoring in Kızılırmak Basin. Türkiye Environ Earth Sci 83:265. https://doi.org/10.1007/s12665-024-11550-0

Şan M (2025) Combined innovative trend analysis methods for seasonal trend testing. J Hydrol 649:132418. https://doi.org/10.1016/j.jhydrol.2024.132418

Saplıoğlu K (2024) Mann-Kendall Trend Testi ile Yenilikçi Yöntemlerin Kıyaslanması: Beşkonak Aylık Akım Verileri Örneği. JICivilTech 6:1–12. https://doi.org/10.60093/jiciviltech.1487245

Schölkopf B, Smola AJ (2002) Learning with Kernels: Support Vector Machines, Regularization, Optimization, and Beyond. MIT Press

Sen PK (1968) Estimates of the Regression Coefficient Based on Kendall's Tau. J Am Stat Assoc 63:1379–1389. https://doi.org/10.2307/2285891

Şen Z (2012) Innovative Trend Analysis Methodology. J Hydrol Eng 17:1042–1046. https://doi.org/10.1061/(ASCE)HE.1943-5584.0000556

Şen Z (2017) Innovative trend significance test and applications. Theor Appl Climatol 127:939–947. https://doi.org/10.1007/s00704-015-1681-x

Şen Z, Şişman E, Dabanli I (2019) Innovative Polygon Trend Analysis (IPTA) and applications. J Hydrol 575:202–210. https://doi.org/10.1016/j.jhydrol.2019.05.028

Sezen C (2023) A new wavelet combined innovative polygon trend analysis (W-IPTA) approach for investigating the trends in the streamflow regime in the Konya Closed Basin, Turkey. Theor Appl Climatol 151:1523–1565. https://doi.org/10.1007/s00704-022-04328-6

Soh YW, Koo CH, Huang YF, Fung KF (2018) Application of artificial intelligence models for the prediction of standardized precipitation evapotranspiration index (SPEI) at Langat River Basin, Malaysia. Comput Electron Agric 144:164–173. https://doi.org/10.1016/j.compag.2017.12.002

Tabari H, Nikbakht J, Hosseinzadeh Talaee P (2013) Hydrological Drought Assessment in Northwestern Iran Based on Streamflow Drought Index (SDI). Water Resour Manage 27:137–151. https://doi.org/10.1007/s11269-012-0173-3

Thornthwaite CW (1948) An Approach toward a Rational Classification of Climate. Geogr Rev 38:55–94. https://doi.org/10.2307/210739

Tuğrul T, Hinis MA (2025) Improvement of drought forecasting by means of various machine learning algorithms and wavelet transformation. Acta Geophys 73:855–874. https://doi.org/10.1007/s11600-024-01399-z

Tuğrul T, Hınıs MA, Oruç S (2025) Comparison of LSTM and SVM methods through wavelet decomposition in drought forecasting. Earth Sci Inform 18:139. https://doi.org/10.1007/s12145-024-01541-x

Varol M, Gökot B, Bekleyen A (2010) Assesment of water pollution in the tigris River in Diyarbakır, Turkey. Water Pract Technol 5:wpt2010021. https://doi.org/10.2166/wpt.2010.021

Vicente-Serrano SM, Beguería S, López-Moreno JI (2010) A Multiscalar Drought Index Sensitive to Global Warming: The Standardized Precipitation Evapotranspiration Index. J Climate 23:1696–1718. https://doi.org/10.1175/2009JCLI2909.1

Wilhite DA, Svoboda MD, Hayes MJ (2007) Understanding the complex impacts of drought: A key to enhancing drought mitigation and preparedness. Water Resour Manage 21:763–774. https://doi.org/10.1007/s11269-006-9076-5

Wong I-S, Ng K-H, Khor K-C (2021) The influence of data preprocessing in predicting Malaysia's GDP growth rate using multilayer perceptron. In: 2021 International conference on Decision Aid Sciences and Application (DASA) (pp 157–160). IEEE

Yalçın S, Eşit M, Çoban Ö (2023) A new deep learning method for meteorological drought estimation based-on standard precipitation evapotranspiration index. Eng Appl Artif Intell 124:106550. https://doi.org/10.1016/j.engappai.2023.106550

Yuce MI, Aytek A, Esit M et al (2025) Investigation of the meteorological and hydrological drought characteristics in yeşilirmak basin. Türkiye Theor Appl Climatol 156:208. https://doi.org/10.1007/s00704-025-05437-8

Zhang Y, Yang H, Cui H, Chen Q (2020) Comparison of the Ability of ARIMA, WNN and SVM Models for Drought Forecasting in the Sanjiang Plain, China. Nat Resour Res 29:1447–1464. https://doi.org/10.1007/s11053-019-09512-6